

Characterization and modeling of THz radiation from USPL-surface interactions

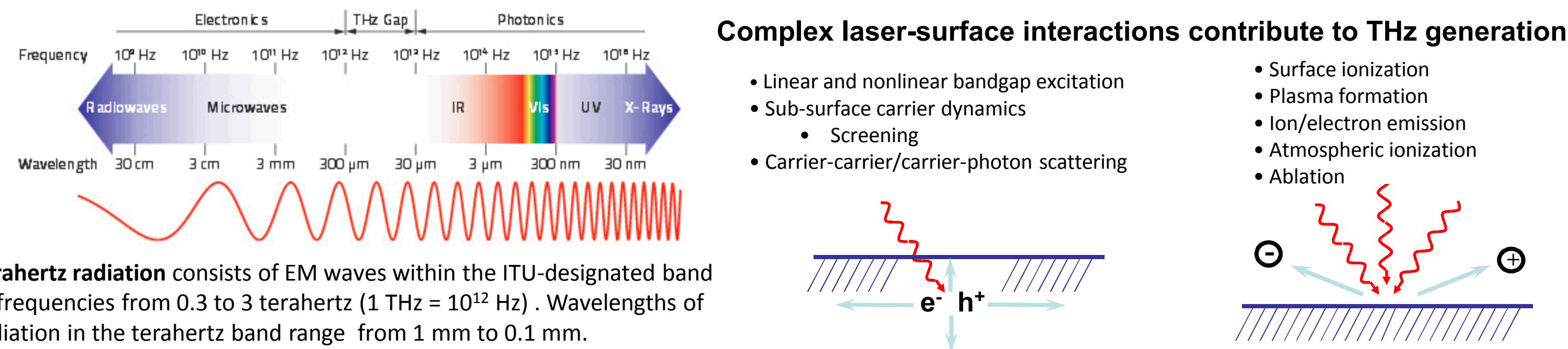
Junji Urayama, Benjamin Yee, Richard Gallegos, Verle Bigman, Fred Zutavern, Weng Chow Sandia National Laboratories, Albuquerque, NM USA 87185

Motivation

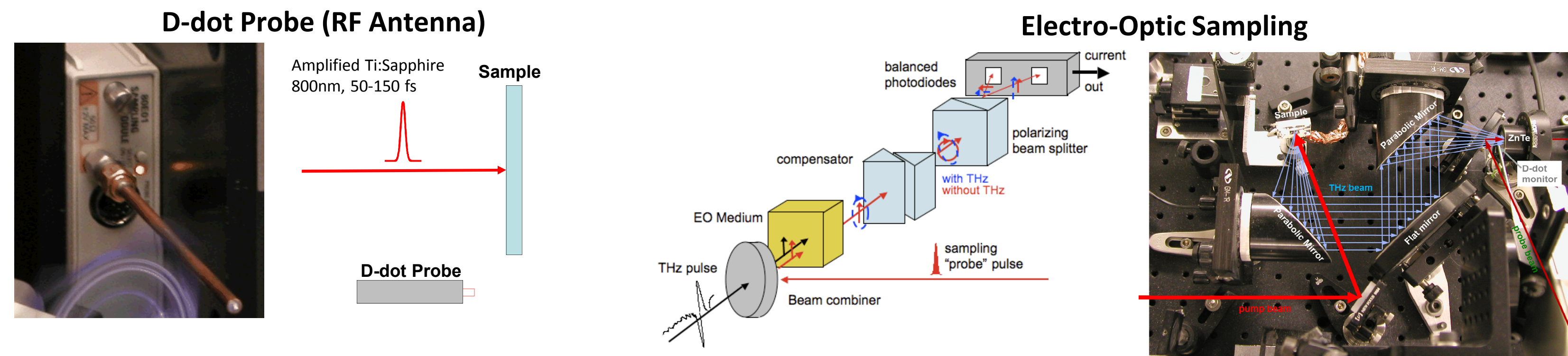
Abstract: It is well known that USPL-surface interactions generate THz radiation. However, the physical mechanisms for THz generation are not fully understood and can vary depending on the surface and incident pulse parameters. This work reports on the THz radiation generated from ultrashort pulses normally incident on surfaces of varying conductivity. In the case of bare samples, the strongest emissions occurred along the plane of the surface, transverse to the incident laser pulse. One cause of these emissions in the surface ionization regime is hypothesized to be the generation of a strong positive space charge layer due to electron emission from the surface or drift/diffusion through the material. Using this assumption, a self-consistent semiclassical theory of dynamical carrier screening was developed which includes the nonequilibrium carrier dynamics within the material and provides a potential explanation for the observed behavior.

Objective: Understand the physical mechanisms that contribute to USPL-induced THz generation by measuring THz field characteristics and modeling underlying mechanisms. Detailed physical understanding may allow for control of THz generation rate and field profile. USPL-induced RF/THz emissions could serve as sources for sensing applications such as imaging, spectroscopy, diagnostics for processes such as micromachining.

THz and USPL Excitation



Experimental Setup: Two Methods



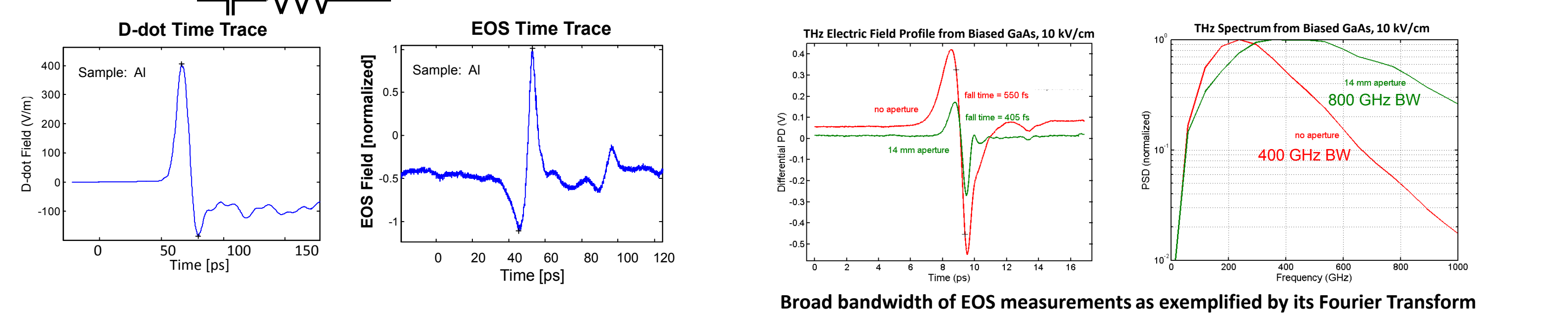
D-dot probes and Electro-Optic Sampling (EOS) are used to measure the THz electric field. The comparison of device characteristics are provided in the table to the right.

	D-Dot	EOS
Measured Quantity	dE/dt	E-field
Bandwidth	70 GHz	~THz
Sensitivity (Min)	50mV/cm	4V/cm
Ease of use	Pro	Con
Configurability	Pro	Con

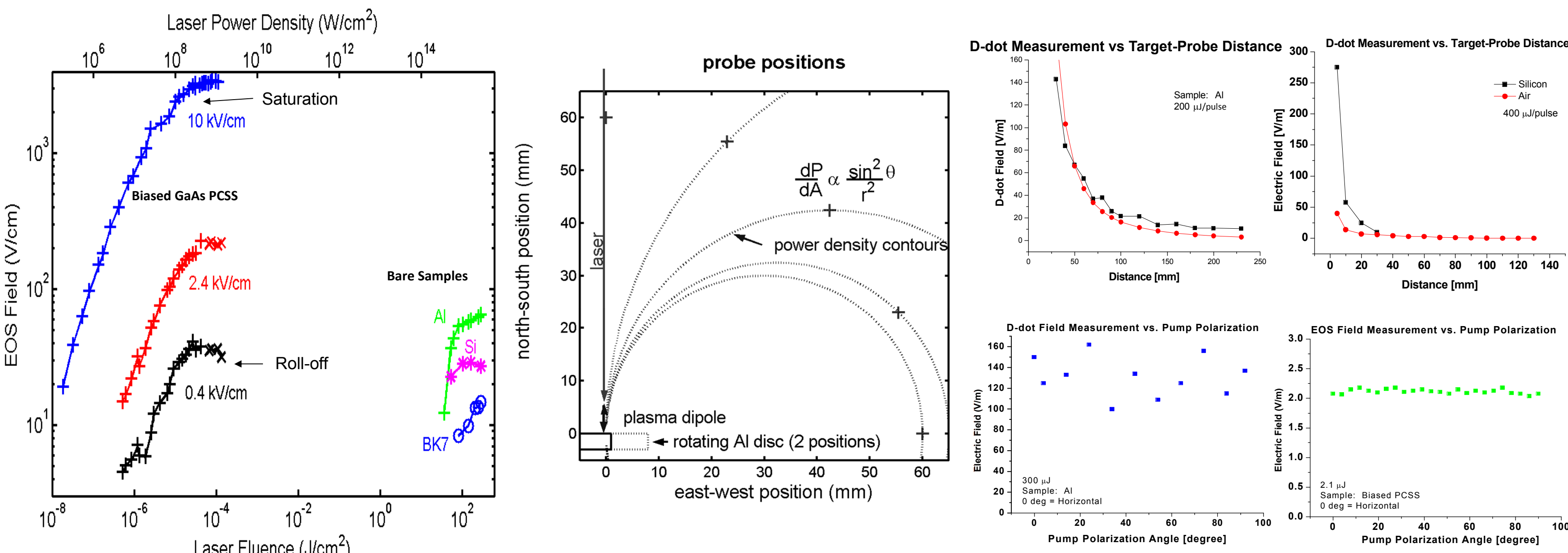
Two types of samples were used as targets:

- Photoconductive switch (biased)
- Bare materials

Experimental Results



Broad bandwidth of EOS measurements as exemplified by its Fourier Transform

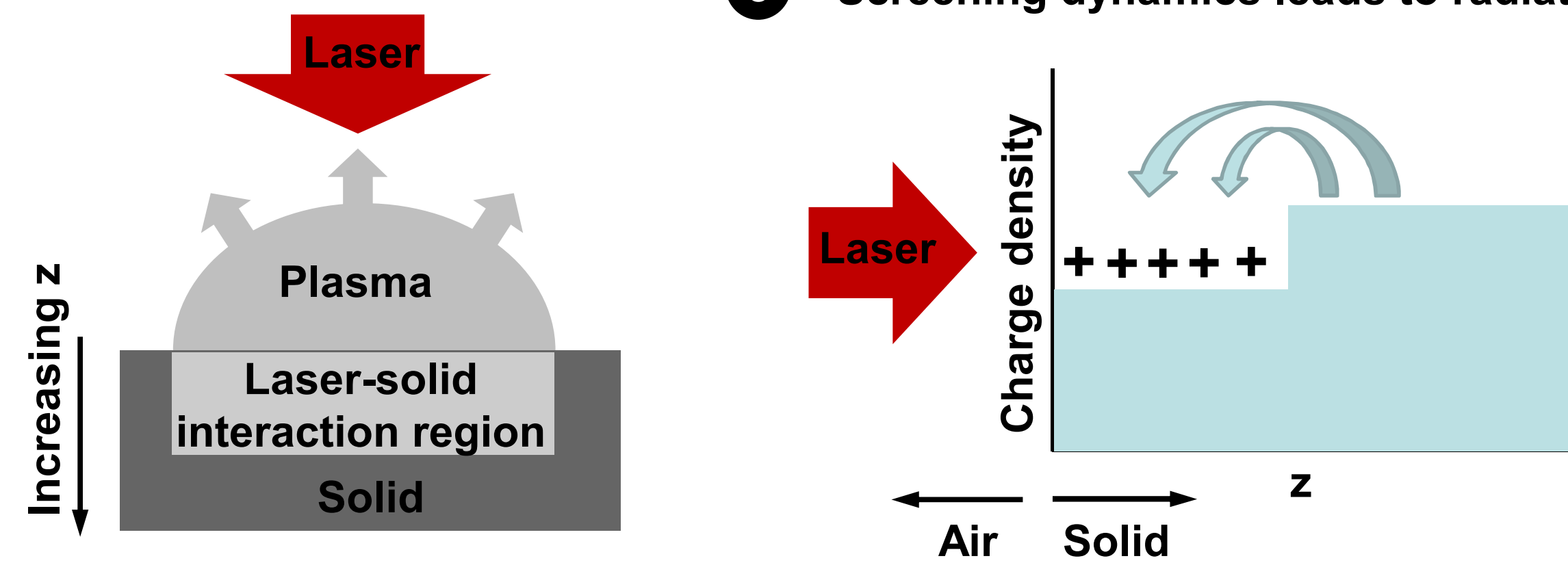


- Biased samples showed 6 orders of magnitude higher response than bare samples
- Emission first increases, saturates, rolls off with increasing laser peak intensity
- Material dependence to emission level observed
- Emission rate decreases with lower ablation rate of material
- Dipole in-plane with surface in PCSS; normal to surface in bare samples
- Emission is laser-polarization independent

Modeling approach

Mechanism

- Laser removes electrons leaving net +ve charge from ions
- Electrons move into depleted region to screen ions
- Screening dynamics leads to radiation



Assumptions

- Spatially averaged laser field and populations within interaction region
- Effective rate equations for scattering effects
- Effective free-carrier absorption interaction Hamiltonian accounting for optical and phonon contributions
- Cluster expansions truncated at singlet level in photon-carrier and carrier-carrier correlations

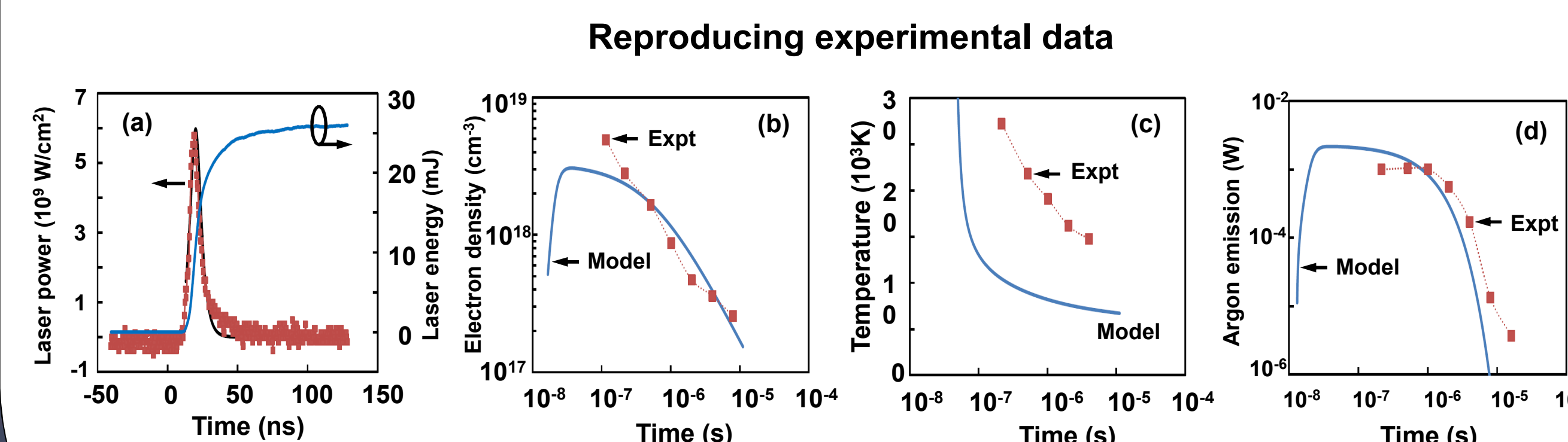
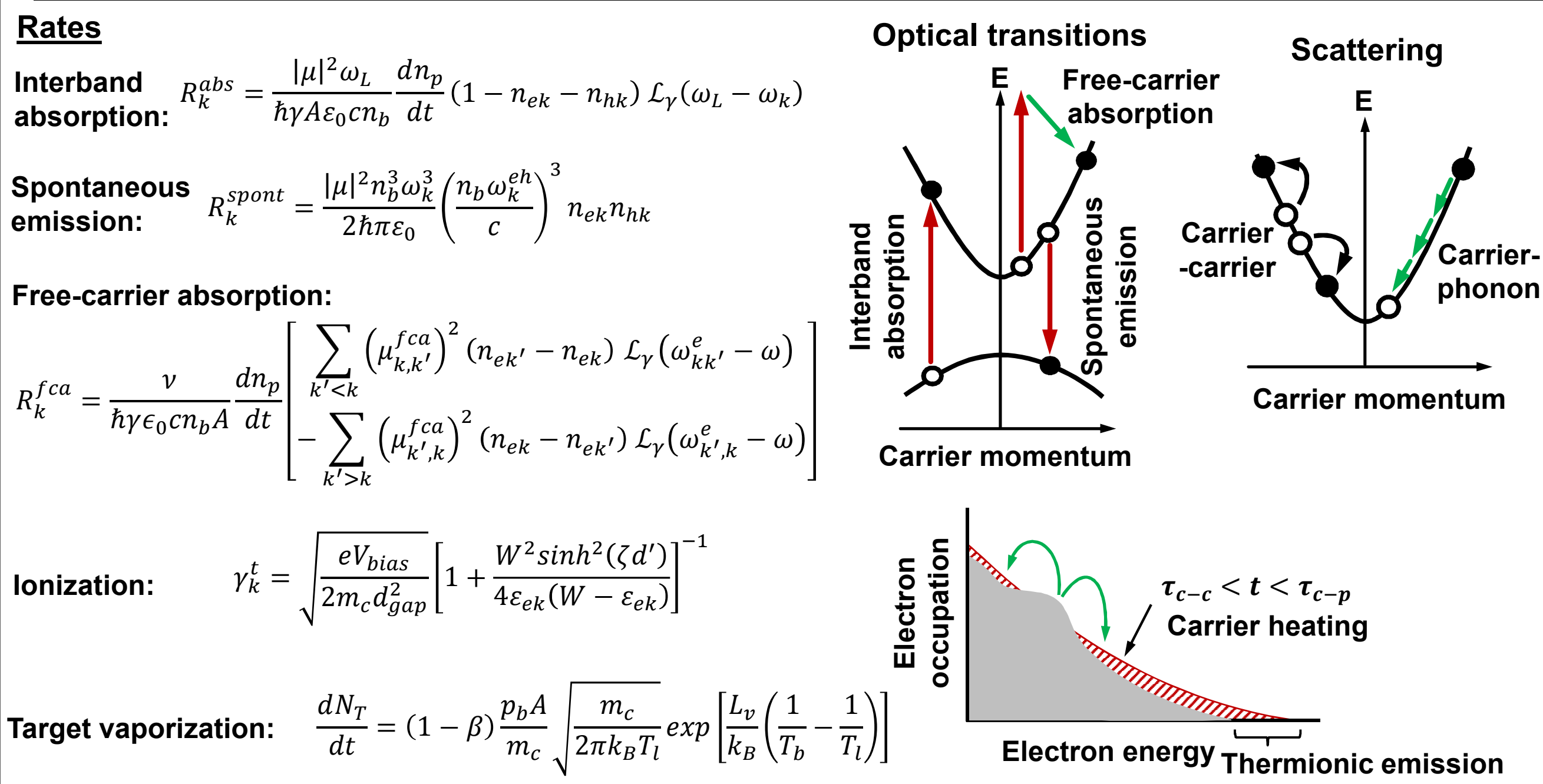
1 Laser-solid interactions

Electrons: $\frac{dn_{ek}}{dt} = R_k^{abs} - R_k^{spont} + R_k^{fca} - \gamma_{c-c}[n_{ek} - f(\epsilon_{ek}, \mu_e, T_c)] - \gamma_{c-p}[n_{ek} - f(\epsilon_{ek}, \mu_e^p, T_p)] - \gamma_k^i n_{ek}$

Holes: $\frac{dn_{hk}}{dt} = R_k^{abs} - R_k^{spont} - \gamma_{c-c}[n_{hk} - f(\epsilon_{hk}, \mu_h, T_c)] - \gamma_{c-p}[n_{hk} - f(\epsilon_{hk}, \mu_h^p, T_p)]$

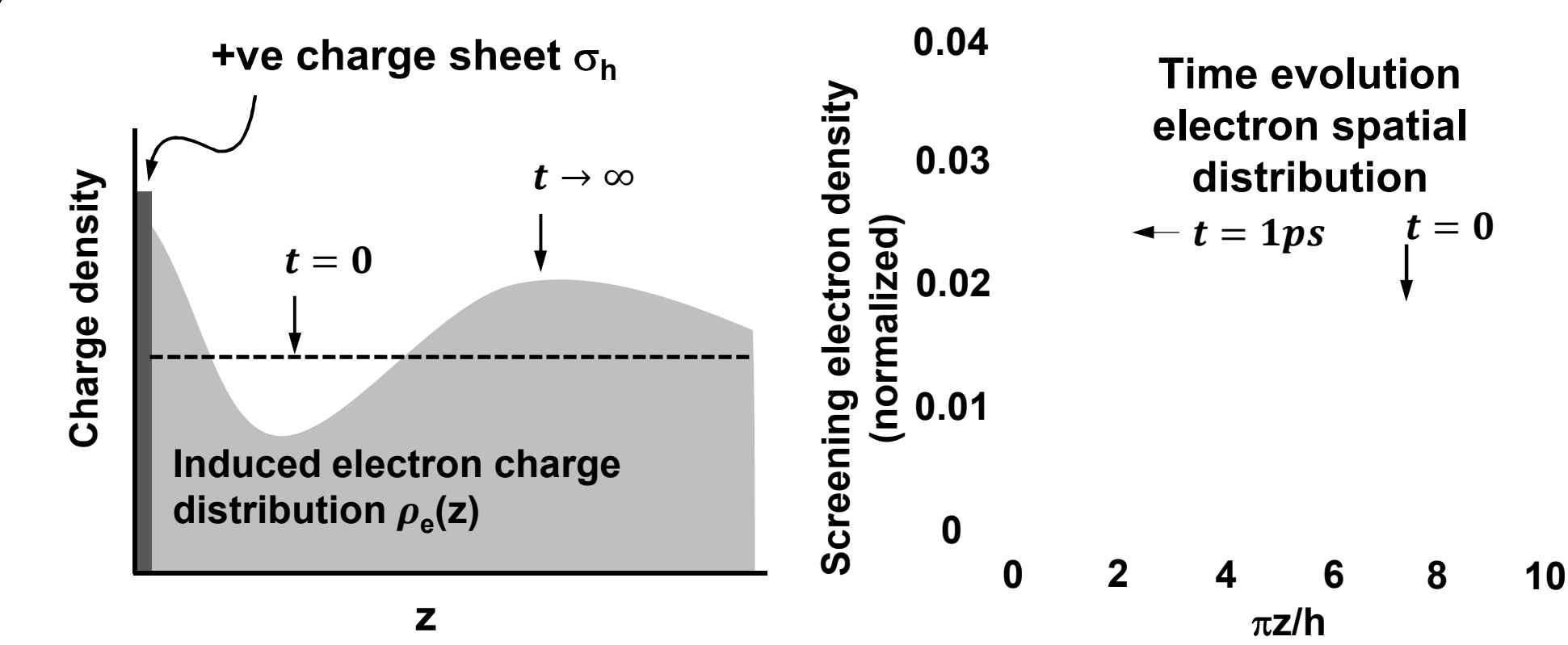
Laser photons: $\frac{dn_p}{dt} = P_p - \sum_k (R_k^{abs} + R_k^{fca})$

Lattice: $C_p \frac{dT_l}{dt} = \gamma_{c-p} \sum_{\sigma=e,h} \sum_k \epsilon_{\sigma k} [n_{\sigma k} - f(\epsilon_{\sigma k}, \mu_l^q, T_l)] - \gamma_c \sum_{\sigma=e,h} \sum_k \epsilon_{\sigma k} [f(\epsilon_{\sigma k}, \mu_l^q, T_l) - f(\epsilon_{\sigma k}, \mu_0^q, T_0)] - L_v \frac{dN_T}{dt}$



Experiment from Xianglei Mao (LBNL)

2 & 3 Screening dynamics



Classical: $E(z) = \frac{e}{2\epsilon_b} \left[\sigma_h(z) - \int_0^z dz' \rho_e(z') \right]$ (Gauss's law)

Screening electron charge distribution: $\rho_e(z) = \langle \hat{\psi}^\dagger(z) \hat{\psi}(z) \rangle = \frac{1}{V} \sum_{k'} \sum_k \langle a_{k'}^\dagger a_k \rangle e^{i(k-k')z}$

Classical \longleftrightarrow Quantum

Quantum mechanics: $H = \sum_k \epsilon_{e,k} a_k^\dagger a_k + \sum_{k'} \sum_k V_{k,k'}^s a_{k'}^\dagger a_k$

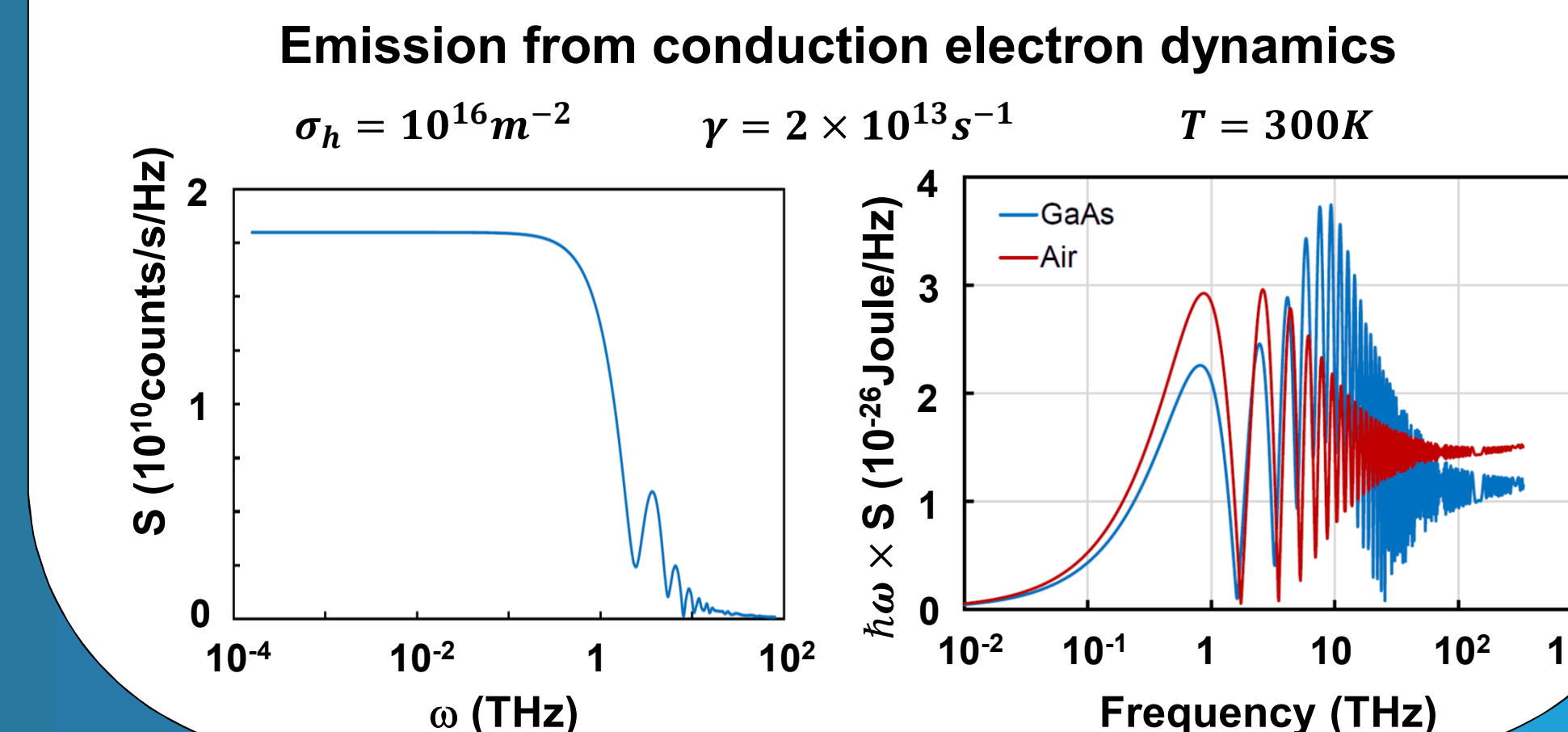
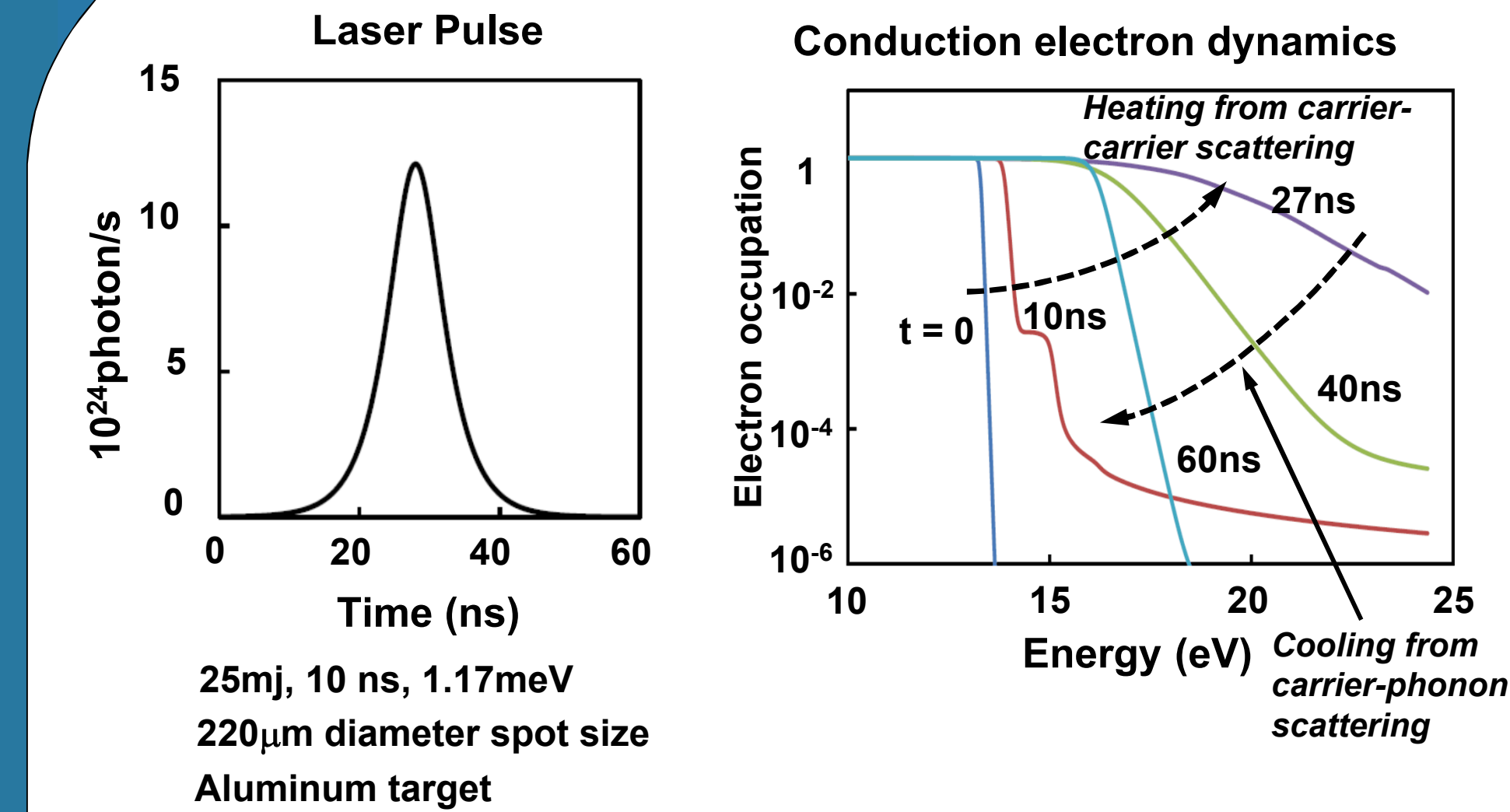
$i\hbar \frac{da_{k'}^\dagger a_k}{dt} = [a_{k'}^\dagger a_k, H]$

$\frac{1}{L} \int_0^L dz V_s(z) e^{i(k-k')z}$

$e \int_0^z dz' E(z')$

Emission spectrum: $S(\omega) \propto \int_0^\infty dt e^{i\omega t} \sum_{k'} \sum_k \langle a_{k'}^\dagger a_k \rangle$

Simulations



Further work

- Develop diagnostics to monitor additional quantities (e.g. plasma, ablation, etc.)
- Complete treatment of THz emission from electron dynamics (determine proportionality constant)
- Combine laser-solid and electron-dynamics calculations
- Connect to experiments
- Refine model based on experiment comparison (reexamine assumptions)
- Optimize THz generation by understanding physical mechanisms